AEGC2019 Data to Discovery
Australasian Exploration Geoscience Conference
2-5 September 2019 • Perth, Western Australia
Incorporating the AIG, ASEG, PESA, and WABS

Fracture identification by reflected guided borehole radar waves

Binzhong Zhou*
CSIRO Energy
PO Box 883
Kenmore, QLD 4069, Australia
Binzhong.Zhou@csiro.au

Jianjian Huo
School of Resources and Environment
University of Electronic Science and
Technology of China, China
huo_jianjian@163.com

Iain Mason
School of Geosciences
The University of Sydney
Sydney 2006, Australia
iain.mason@sydney.edu.au

Qing Zhao
School of Resources and Environment
University of Electronic Science and
Technology of China, China
zhaoq@uestc.edu.cn

SUMMARY

Reflected guided borehole radar waves can be observed when a borehole radars (BHR) is either suspended by a conductive communication cable or run in a borehole filled with saline water. They are often referred as unwanted contaminations to the conventional BHR surveying and should be avoided or suppressed. However, as a type of reflected waves, they contain geological information about the surroundings of the borehole and can be used to recognise geological boundaries such as lithological interfaces and fractures intersecting the borehole. The guided BHR reflections have different phase characteristics for stratigraphic boundaries and fractures. The reflections from both sides of a fracture have the same phase, whereas the reflections from both sides of a stratigraphic interface have opposite phases. Such characteristics enable us to differentiate fractures from bedding boundaries down the borehole using the borehole guided waves. This is demonstrated by both synthetic and real field data.

Key words: fracture identification, borehole radar, guided wave

INTRODUCTION

Borehole radar (BHR) is an effective imaging tool for subsurface investigation. It can be used in two modes: single-hole reflection (transmitter and receiver in the same borehole) and tomographic cross-hole transmission (transmitter and receiver in separate boreholes) (Zhou and Fullagar, 2001). It has been applied to cavity, void and tunnel detection (Kim et al., 2004, 2010), fault and fracture mapping (Olsson et al., 1992), coal seam exploration (Cook, 1977), stratigraphic mapping within salt mines (Eisenburger et al., 1993), hydrological property mapping (Deiana et al., 2007), geotechnical evaluation (Mason et al., 2012), orebody delineation (Turner et al., 2000), burning front detection during coal gasification (Davis et al., 1979), monitoring enhanced oil recovery processes (Laine, 1987) and ice property analysis (Axtell et al., 2016). Borehole radar, correctly applied, can contribute to the understanding of subsurface fractures, help to predict and reduce mining risks, and be used to monitor potential geological hazards.

In single-hole reflection mode, BHR is used to map subsurface structures such as the lithologic boundaries and fractures parallel or sub-parallel to the axis of the borehole. Interfaces sub-perpendicular to the borehole are harder to see, because axial dipole antennas launch electromagnetic (EM) waves radially. They have an axial EM wave radiation null. However, structures perpendicular or sub-perpendicular to the borehole are almost always of interest and they need to be mapped.

We have found (Mason et al., 2008; Zhou and van de Werken, 2015; Mao and Zhou, 2017) that if a BHR is attached to a conductive wire or runs in a conductive saline water-filled borehole, then reflected guided borehole radar waves, travelling along the borehole, are often recorded. They can interfere with normal BHR surveys and can be suppressed (Huo et al., 2018). However, drill-string guided BHR waves can be used for seeing ahead of the drill-bit (Zhou and van de Werken, 2015; Mao and Zhou, 2017; Zhou and Madden, 2018) and detecting geological interfaces especially for those interfaces sub-perpendicular to the borehole (Mason et al., 2008; Zhou and van de Werken, 2015).

Guided BHR reflections from planar structures like lithological boundaries and fractures can not only be used for detecting those interfaces sub-perpendicular to the borehole, but can also be used to differentiate fractures from bedding boundaries along the borehole. This will be demonstrated here using synthetic and real field data.

METHOD

When a BHR is attached to conductive cables at its top and bottom or is operated in a borehole filled with conductive mud or water, both up- and down-going waves guided by the borehole will be induced (Mason et al., 2008; Zhou and van de Werken, 2015). When guided waves, travelling along the borehole, hit geological discontinuities, they may be reflected, then detected by the BHR receiver. Guided waves create “V” shaped patterns on BHR profiles (Mason et al., 2008; Zhou et al., 2015). The arms of the V are formed by the up- and down-going reflections from either side of a boundary, as illustrated in Figure 1. The reflected waves can be used to identify geological boundaries such as lithological interfaces and fractures intersecting the borehole. Figure 1 shows that the reflections from both sides of a fracture are of the same phase while the reflections from both sides of a bedding plane have opposite phases. The absence or presence of phase changes helps to distinguish between fractures and bedding planes that intersect the borehole.

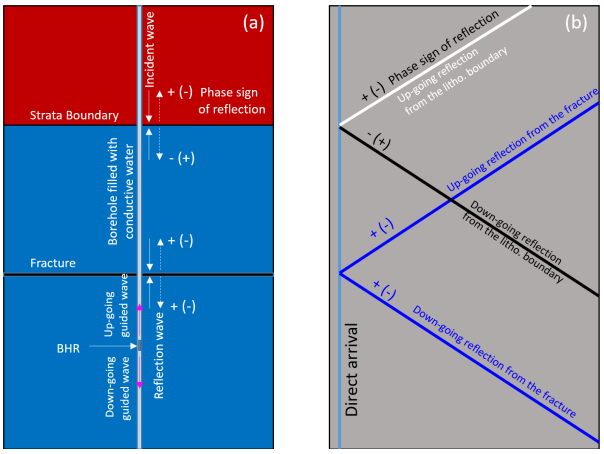

Figure 1. Illustration of the phase differences of guided reflections from a lithological boundary and a fracture. (a) Geological model with a fracture and a lithological boundary. (b) Detected guided reflections from the lithological boundary and the fracture. The reflections from both sides of a fracture have the same phase sign while the reflections from both sides of a stratigraphic interface have opposite phases.

RESULTS

Numerical Example

Figure 2a shows a three-layered model with two lithological boundaries ① and ⑨, six horizontal fractures ②-④ and ⑥-⑧, and a cavity ⑤. Except for the fracture ②, the borehole passes through all boundaries perpendicularly. The borehole has a diameter of 0.2 m and is filled with conductive water. The fractures and cavity are filled with the same water. Relevant permittivities and conductivities are marked on the plot.

A mono-static BHR - in which the transmitter Tx and receiver Rx share the same antenna - travels in steps of 0.05 m along a borehole. The Tx fires a pulse with a Gaussian envelope of ~2.2 ns half-width with a 200 MHz centre frequency. The recording time length per trace is 60 ns. Figure 2b shows the original synthetic mono-static BHR profile from the model in Figure 2a, with very strong direct arrivals dominated from the Tx. A moving average error filter with a length of 7 traces is applied to the original data (Figure 2b) in order to suppress the direct waves and enhance the other signals (Huo et al., 2018). The processed result is displayed in Figure 2c, in which guided wave reflections from the fractures and boundaries intersected by the borehole create obvious V-shapes. However, no reflections are observed from fracture ② and cavity ⑤ because they are situated away from the borehole. Borehole water conductivity shields radiation of the side-looking EM wave from the antenna. Up- and down-going guided wave reflections from the lithological boundaries ① and ⑨ have opposite phases; whilst up- and down-going guided wave reflections from fractures have the same phase. It follows that phase changes or their absence can be used to differentiate borehole intersections with bedding planes and fractures.

Field Data Example

Figure 3 shows a real data example. The raw bi-static BHR profile in Figure 3a is a part of the data acquired from a 60 mm borehole in Canada filled with very conductive water. The data gather is displayed after a static time shifting to convert bi-static data into pseudo-mono-static data. The Tx and Rx have a broadband asymmetric dipole antenna with an efficient frequency range of 25-150 MHz. The offset between Tx and Rx is 0.5 m. As the radar moves down the borehole, traces are stacked, and recorded at ~0.15 m spatial intervals. Each recorded trace is 1.022 μs long with a time sampling rate of 0.002 μs.

V-shaped borehole guided events observed on the raw section (Figure 3a) are obstructed by strong direct arrivals and vertical stripes. A moving average error filter of 21-traces suppresses both direct arrivals and vertical stripes in the raw data (Figure 3a). The filtered result is displayed in Figure 3b with an Automatic-Gain Control (AGC) of 0.05 μs. Borehole guided V-shaped patterns are now clearly displayed. Rocks in this section of the borehole are relatively uniform according to the geological log for the borehole. The Rock Quality Designation (RQD) log indicates some defects. Based on this information, we can confidentially say the V-shaped event at ~70 m relates to a lithological boundary because the two branches of the reflections have opposite phases. All other V-shaped borehole guided events have the same phase signs for their corresponding reflection branches, indicating that they are associated with fractures.

CONCLUSIONS

Fractures are important geological features for geotechnical investigation of the suitability of the host rock for example, nuclear waste storage, groundwater movement pathways and oil recovery method designs. In this paper, we advocate that borehole guided EM waves can be used to distinguish fractures from rock boundaries. Both synthetic and real field data demonstrate the feasibility of the proposed approach. The presence or absence of phase changes at the apex of the V-shape can also be used to diagnose normal borehole radar data if planes intersect the borehole at acute angles.

ACKNOWLEDGEMENTS

The Australian Coal Association Research Program (ACARP) under Grant C26022, and China Scholarship Council under the State Scholarship Fund No. 201706070106, and International Cooperation, Science and Technology Department of Sichuan Province, China (Grant no. 18GJHZ0037), are thanked for their support to this research. Dr Kevin Smith is thanked for acquiring the field data used in this paper.

REFERENCES

Axtell, C., Murray, T., Kulessa, B., Clark, R.A., and Gusmeroli, A., 2016, Improved accuracy of cross-borehole radar velocity models for ice property analysis: Geophysics, vol. 81, no. 1, pp. WA203–WA212.

Cook, J.C., 1977, Borehole exploration in a coal seam: Geophysics, vol. 42, no. 6, pp. 1254–1257.

Davis, D.T., Lytle, R.J., and Lame, E.F., 1979, Use of high-frequency electromagnetic waves for mapping an in situ coal gasification burn front," In Situ, vol. 3, no. 2., pp.95–119.

Deiana, R., Cassiani, G., Kemna, A., Villa, A., Bruno, V., and Bagliani, A., 2007, An experiment of non-invasive characterization of the vadose zone via water injection and cross-hole time-lapse geophysical monitoring: Near Surface Geophysics, vol. 5, no.3, pp. 183–194.

Eisenburger, D., Sender, F., Thierbach, R., 1993, Borehole radar —an efficient geophysical tool to aid in the planning of salt caverns and mines: Seventh Symposium on Salt, vol. 1, pp. 279–284.

Huo, J., Zhou, B., Zhao, Q., Mason, I., 2018, Suppressing reflected guided waves from contaminated borehole radar data: IEEE Geoscience and Remote Sensing Letters (in press). Doi:10.1100/LGRS.2018.2880753.

Kim, J. H. , Cho, S. J., and Yi, M. J., 2004, Borehole radar survey to explore limestone cavities for the construction of a highway bridge: Exploration Geophys., vol. 35, no. 1, pp. 80–87.

Kim, S. W., Kim, S. Y., and Nam, S., 2010, Estimation of the penetration angle of a man-made tunnel using time of arrival measured by shortpulse cross borehole radar: Geophysics, vol. 75, no. 3, pp. 11–18.

Laine, E.F., 1987, Remote monitoring of the steam-flood enhanced oil recovery process: Geophysics 52, 1457-1465.

Mao, L., and B. Zhou, 2017, Simulation and Analysis of Conductively Guided Borehole Radar Wave: IEEE Transaction on Geoscience and Remote Sensing, Vol 55, No. 5, 2646-2657.

Mason, I.M., Bray, A.J., Sindle, T.J., Simmat, C.M., and Cloete, J.H., 2008, The effect of conduction on VHF radar images shot in water-filled boreholes: IEEE Geosci. Remote Sens. Lett., vol. 5, no. 2, pp. 304-307.

Mason, I.M., Cloete, J.H., and Palmer, K.D., 2012, Borehole radar imaging in tactical support of miners working in very narrow stopes: in 2012 IEEE-APS Topical Conference on Antennas and Propagation in Wireless Communications (APWC), pp. 973–976.

Olsson, O., Falk, L., Forslund, O., Lundmark, L., and Sandberg, E., 1992, Borehole radar applied to the characterization of hydraulically conductive fracture zones in crystalline rock: Geophysical Prospecting, 40, 109-142.

Turner, G., Mason, I.M., Hargreaves, J., and Wellington, A., 2000, Borehole radar surveying for orebody delineation: in Proceedings of the International Conference on Ground Penetrating Radar, Gold Coast, Australia, pp. 282–287, 23–36.

Zhou, B. and Fullagar, P.K., 2001, Delineation of sulphide ore-zones by borehole radar tomography at Hellyer Mine, Australia: J. Appl. Geophys., vol. 47, no. 3/4, pp. 261–269.

Zhou, B., and Madden, R., 2018, Detection of top coal by conductively-guided borehole radar waves: results from numerical modelling: Proceeding of the 17th International Conference on Ground Penetrating Radar (GPR), Rapperswil, Switzerland, June 18-21, 2018.

Zhou, B. and van de Werken, M., 2015, Conductively guided borehole radar wave for imaging ahead of a drill bit: IEEE Geosci. Remote Sens. lett., vol. 12, no. 8, pp. 1715-1719, Aug. 2015.

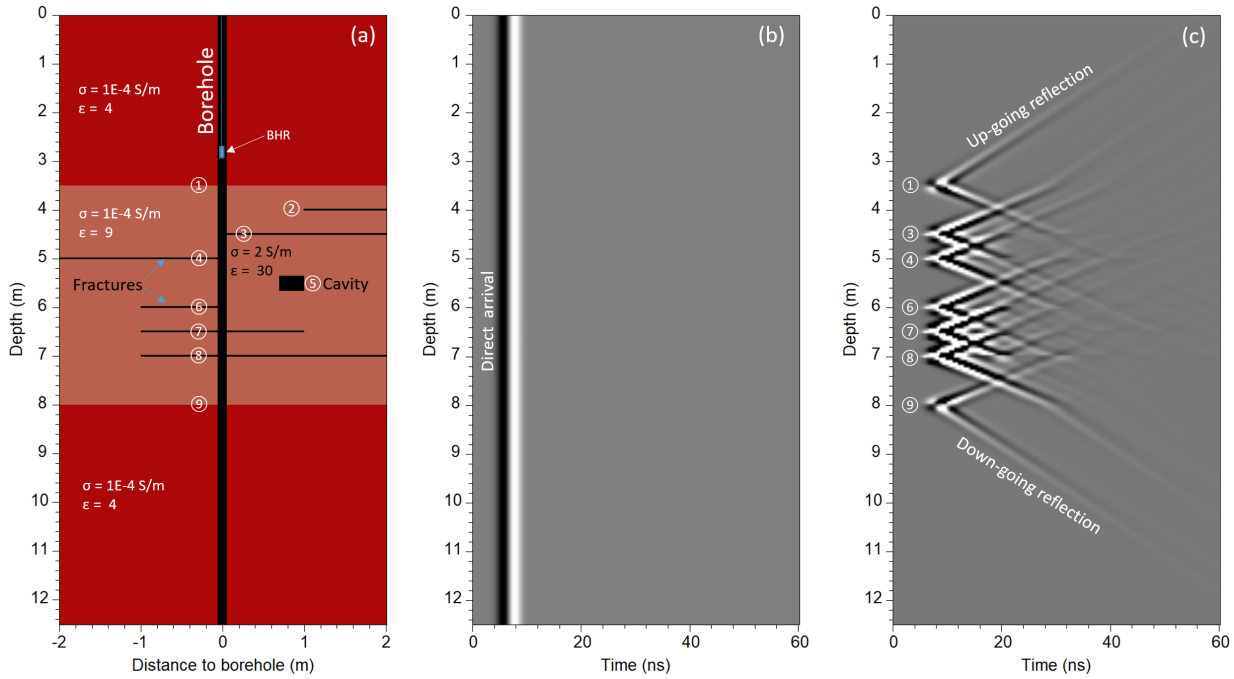

Figure 2. Numerical example of fracture detection by guided BHR waves: (a) Geological model; (b) mono-static BHR profile corresponding to the model (a); (c) Reflected guided BHR waves associated with the lithological boundaries and fractures after suppressing the direct arrival in (b).

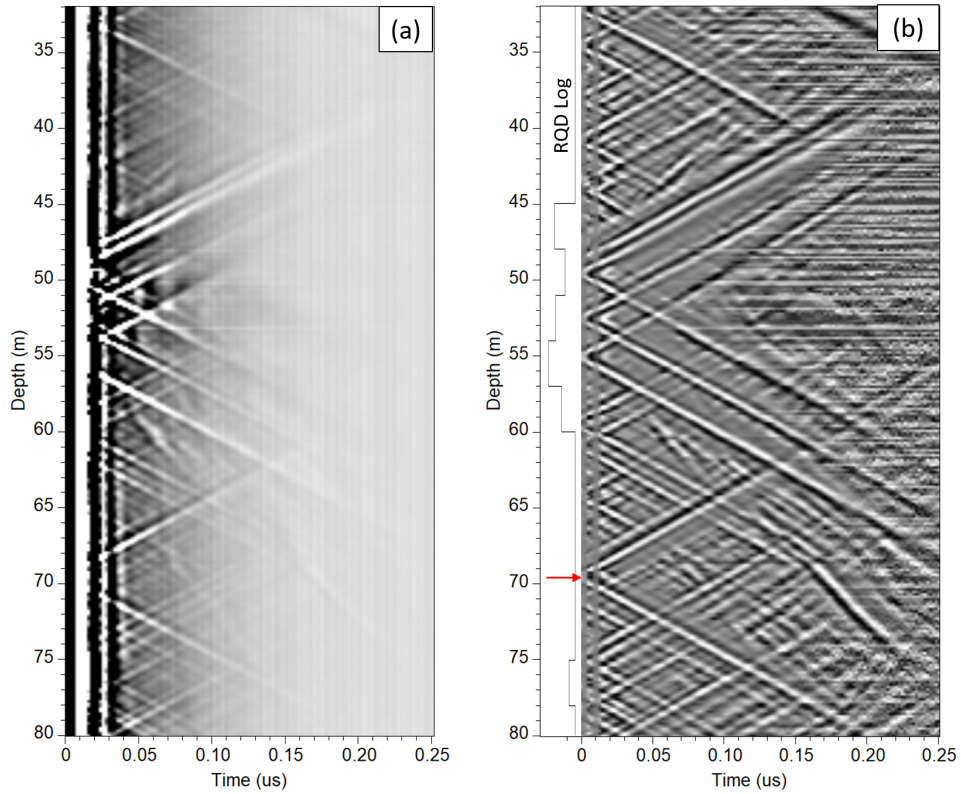

Figure 3. Real BHR data example acquired from a borehole filled with conductive water (high salinity): (a) Raw bi-static BHR profile with borehole guided waves; (b) Enhanced guided wave events, after suppressing the direct arrivals and with 0.05 µs AGC applied. The RQD log in (b) has a high value to the right.